JOURNAL OF APPLIED ELECTROCHEMISTRY 18 (1988) 245–251

Use of the Nasicon/Na_2SO_4 couple in a solid state sensor for $SO_x (x = 2, 3)$

R. AKILA, K. T. JACOB

Department of Metallurgy, Indian Institute of Science, Bangalore 560 012, India

Received 22 July 1987

The e.m.f. of a concentration cell for $SO_x (x = 2, 3)$-O_2 incorporating Nasicon as the main solid electrolyte has been measured in the temperature range 720 to 1080 K. The cell arrangement can be represented as,

$$Pt, O_2' + SO_2' + SO_3' | Na_2SO_4 || Nasicon || Na_2SO_4 | SO_3'' + SO_2'' + O_2'', Pt$$

The Na_2SO_4 acts both as an auxiliary electrode, converting chemical potentials of SO_x and O_2 to equivalent sodium potentials, and as an electrolyte. The presence of Na_2SO_4 provides partial protection of Nasicon from chemical reaction with gas mixtures containing SO_x. The open circuit e.m.f. of the cell is in close agreement with values given by the Nernst equation. For certain fixed inlet gas compositions of $SO_2 + O_2$, the e.m.f. varies non-linearly with temperature. The intrinsic response time of the cell to step changes in gas composition is estimated to vary from ~ 2.0 ksec at 723 K to ~ 0.2 ksec at 1077 K. The cell functions well for large differences in partial pressures of $SO_3 (p''_{SO_3}/p'_{SO_3} \approx 10^4)$ at the electrodes.

1. Introduction

Oxides of sulphur are produced as gaseous pollutants during combustion of fossil fuels and during non-ferrous smelting. It is necessary to monitor the concentration of these gases escaping into the atmosphere both for process control and reduction of environmental polution. Solid state sensors for SO_x are therefore of great interest as they operate at high temperatures and can be used *in situ* for industrial stack gas analysis. When produced in large numbers, solid state sensors are expected to be more economic than conventional methods based on chromatography and infrared analysis.

The high temperature form of alkali sulphates $M_2SO_4 (M = K, Na, Li)$ have been used as solid electrolytes in sensors for $SO_x (x = 2, 3)$ species [1–6]. Gauthier *et al.* [1] employed K_2SO_4 as the electrolyte, while Jacob and Rao [2] used Na_2SO_4. Later, Liu and Worrell [3–5] experimented with Li_2SO_4 and Li_2SO_4 doped with 5 mol% Ag_2SO_4. Saito *et al.* [6] have used Na_2SO_4 doped with $Y_2(SO_4)_3$. Different reference electrodes have been used with the alkali sulphate electrolytes – gaseous electrodes consisting of $O_2 + SO_2 (+ SO_3)$, $Ag + Ag_2SO_4$ with Ag_2SO_4 dissolved in the alkali sulphates, an air reference with $M_2SO_4 |$ $(CaO)ZrO_2$ junction, and oxide-sulphate mixtures [1–8]. The response times of sensors based on alkali sulphates varies between 0.2 to 0.4 ksec at 973 K [1–5]. The phase transformation from the low to the high temperature form of alkali sulphates is accompanied by large enthalpy and volume changes. When the sulphates are cycled rapidly and repeatedly through the transformation temperature, microcracks develop in the solid electrolyte. Although the cracks heal under a small compressive stress when heated above ~ 1100 K, in some applications such *in situ* heat treatment may be inconvenient. The presence of interconnecting microcracks can lead to gas permeation and lowering of the e.m.f.

Among alkali sulphates, the enthalpy of phase transformation is larger for Li_2SO_4 than for the other sulphates. Lithium sulphate also exhibits higher reactivity to silica used in cell construction compared to the other alkali sulphates. Potassium sulphate exhibits the lowest conductivity because of its larger ionic radius. At high partial pressures of SO_3, K_2SO_4 converts to a liquid phase rich in pyrosulphate [2]. From the point of view of conductivity, transformation enthalpy, phase stability and sinterability, Na_2SO_4 appears to be the most promising material among sulphates. Imanaka *et al.* [9] have shown that the phase transformation in Na_2SO_4 can be suppressed by mixing with Li_2SO_4, $Y_2(SO_4)_3$ and SiO_2, without any adverse effect on ionic conductivity. Jacob *et al.* [10] have recently used CaF_2 solid electrolyte along with $CaSO_4$ as the auxiliary electrode for measurement of SO_x. However, the cell exhibited a slow response time, ~ 7 ksec at 1200 K.

Maruyama *et al.* [11] have used Nasicon as a solid electrolyte in a sensor for SO_x in the temperature range 929 to 1124 K. A thin adherent layer of Na_2SO_4 was formed *in situ* on Nasicon by reaction with the gas phase. Once a layer of Na_2SO_4 is formed, the rate of reaction is slow. Since Na_2SO_4 is a Na^+ ion conductor [2], diffusion flux through this material is limited by the trace concentration of electrons or holes. However if the cell is cycled through the phase transformation

0021-891X/88 $03.00 + .12

temperature for Na_2SO_4, cracks develop in the protective layer, providing direct access for the gas phase to the Nasicon. Under such conditions, Na_2O from the electrolyte is continuously consumed, causing composition changes and mechanical deterioration of the solid electrolyte over long exposures. This problem can be partly overcome by covering the Nasicon with a dense envelope of Na_2SO_4 which acts both as an auxiliary electrode and as a solid electrolyte. This paper reports studies on the Nasicon|Na_2SO_4 couple for the measurement of SO_x species in gases.

2. Experimental details

2.1. *Materials*

The Nasicon ($Na_3Zr_2Si_2PO_{12}$) was prepared by reacting an intimate mixture of fine powders of $ZrSiO_4$, Na_2CO_3, ZrP_2O_7 and Na_2SiO_3 in the ratio 1.5 : 1 : 0.5 : 0.5 at 1473 K for a total of ~ 200 ksec in tightly closed Pt containers. The purity of the chemicals used was better than 99.9%. After intervals of ~ 50 ksec, this mixture was cooled to room temperature, reground and repelletized for further heat treatment. With this procedure, single phase Nasicon of the desired composition could be prepared without any trace of $ZrSiO_4$ or ZrO_2 in X-ray diffraction patterns.

The anhydrous Na_2SO_4 powder used in this study was 99.99% pure. Gas mixtures (numbers 1 to 3) were prepared by mixing separate metered streams of dry high purity SO_2, O_2 and Ar in a glass tower packed with glass beads. The flow rates of the gases were controlled by a Matheson multiple mass flow controller (model 8249). Gas mixtures (numbers 4, 5 and 10) were prepared by admitting SO_2 into cylinders containing O_2 + Ar mixtures. The concentration of O_2 in the Ar + O_2 mixture prior to admission of SO_2 was determined using an oxygen sensor based on $(CaO)ZrO_2$. The concentration SO_2 in the final mixture was determined by chemical analysis.

2.2. *Apparatus*

A schematic diagram of the apparatus is shown in Fig. 1. The cell consists of two identical parts. Each part was assembled using a pellet of Nasicon, having polished flat surfaces, spring loaded against a vertical silica tube with a gold O-ring in between. A retaining ring was placed around the assembly to prevent lateral displacement of the silica tube with respect to the Nasicon pellet. Sodium sulphate powder was rammed tightly against the Nasicon pellet inside the silica tube and was sintered *in situ* at 1080 K for ~ 40 ksec. The cell was assembled by pressing together the two half cells with their Nasicon discs in contact. A fine platinum mesh was placed on the surface of the Na_2SO_4 and platinum leads were attached to the mesh. The mesh was held against the Na_2SO_4 by the gas outlet tube. Coiled platinum catalysts were hung on hooks on the outside of the gas outlet tube to bring the incoming gas into thermodynamic equilibrium. The test gas was passed through the top half cell, while the

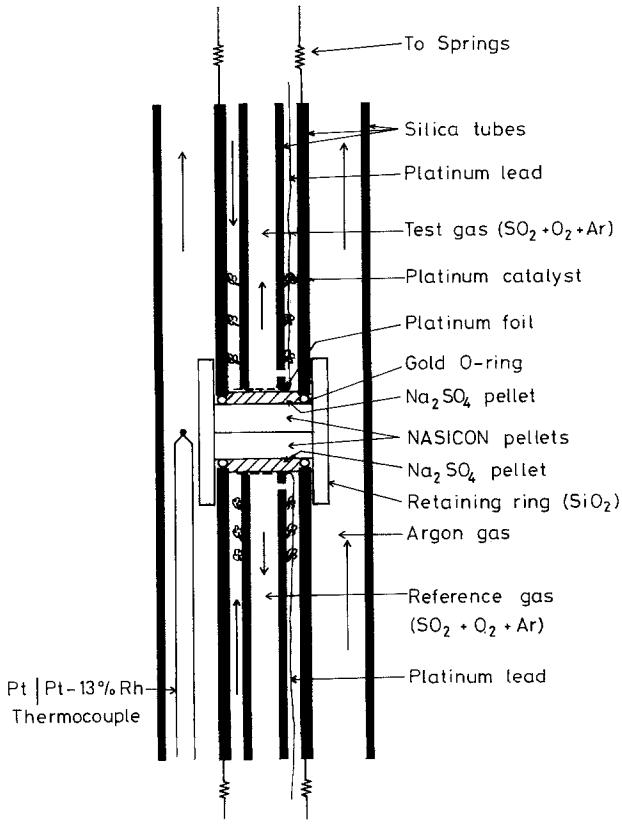

Fig. 1. Schematic representation of cell arrangement.

reference gas (No.4) flowed through the bottom part of the cell assembly. The entire assembly was enclosed in an outer vertical silica tube through which purified argon gas was passed at a flow rate of 5 ml sec^{-1}.

Preliminary experiments indicated that at low temperatures (T < 850 K) the wire catalysts at the gas inlet were not sufficient to ensure thermodynamic equilibrium in the gas phase. The gases were therefore pre-equilibrated in a separate furnace containing honeycomb catalyst and maintained at the same temperature (± 1 K) as the cell used for the e.m.f. studies. The temperatures were measured with Pt/Pt-13% Rh thermocouples.

The top and bottom of the outer silica tube enclosing the cell assembly were closed with water cooled brass heads provided with O-rings to ensure gas tightness. The brass heads had provisions for holding the silica gas outlet tubes, inlets for gases, connectors for electric leads and thermocouples and attachments for springs. The outer silica tube enclosing the cell was suspended inside a vertical Kanthal furnace with the brass heads projecting outside. The cell leads were shielded from induced e.m.f. by an earthed stainless steel sheet wrapped around the outer silica tube. The temperature of the furnace was controlled to ± 1 K by a Thyristor power controller.

2.3. *Procedure*

The e.m.f. of the cell,

$$Pt, O_2' + SO_2' + SO_3' \,|\, Na_2SO_4 \,\|\, \text{Nasicon} \,\|\, Na_2SO_4 \,|\, SO_3'' + SO_2'' + O_2'', Pt - I$$

was measured as a function of temperature in the range 720–1080 K. The cell assembly was initially heated to 1000 K. The reference and test gas compartments were evacuated one at a time, maintaining the pressure inside the outer silica tube at 1 atm. Gas leakage through the gold O-rings was found to be negligible under these conditions. The flow rate of the reference and test gases was varied between 2 and 6 ml sec^{-1}. The cell e.m.f. was independent of flow rate in this range. The flow rates through both compartments were maintained at approximately the same value to avoid thermal gradients across the electrolyte due to preferential cooling by the gas. The reversibility of the cell was checked by coulometric titration. The cell e.m.f. returned to the initial value after passing small currents (~ 100 A for ~ 200 sec) through the cell in either direction. The measured e.m.f.s were reproducible on temperature cycling.

3. Results

The open circuit e.m.f. of cell I is plotted in Figs 2 and 3 as a function of temperature. Fig. 2 gives the variation of e.m.f. with temperature for test gases 1, 2 and 3 while Fig. 3 shows corresponding data for test gases 5 and 10. The e.m.f. varied non-linearly with temperature. Test gas 5 showed a peak at 900 K. Table 1 gives the measured e.m.f.s and response times ($t_R = t_{0.99}$) of cell I for the different test gases. This response time includes the time required for the experimental system to be flushed by the new gas mixture. It is estimated that ~ 300 sec are needed to establish a new partial pressure at the electrodes after a step change in gas composition. Therefore intrinsic response times may be smaller than that indicated in Table 1 by 300 sec.

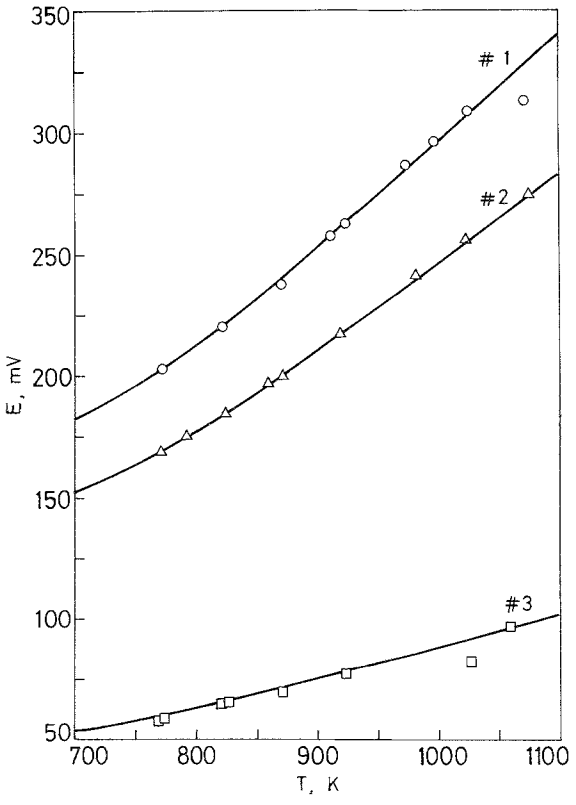

Fig. 2. Variation of e.m.f. with temperature for test gases 1, 2 and 3.

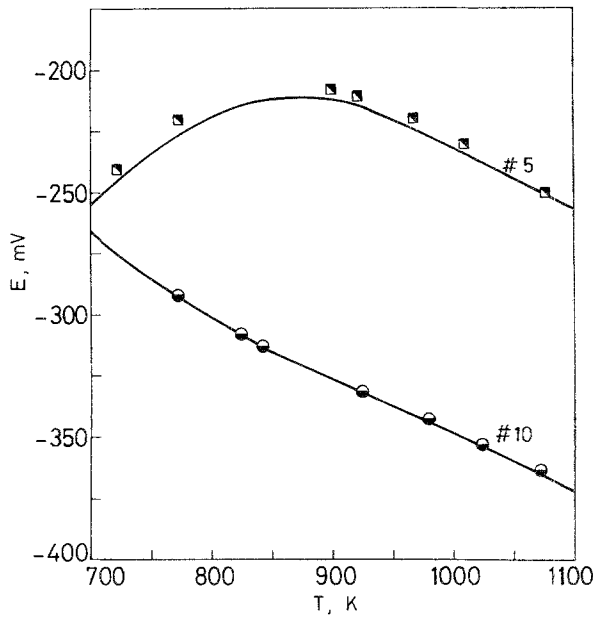

Fig. 3. Dependence of e.m.f. on temperature for test gases 5 and 10.

4. Discussion

4.1. *Cell reaction*

Since Nasicon and Na_2SO_4 are established sodium ion conductors, a cell employing these electrolytes will respond to the difference in the chemical potentials of sodium at the electrodes. At equilibrium, the electrochemical potential of sodium $\tilde{\mu}_{Na^+}$ is uniform throughout the electrolyte. Thus,

$$\tilde{\mu}'_{Na^+} = \tilde{\mu}''_{Na^+} \tag{1}$$

where $'$ and $''$ denote anode and cathode respectively. The electrochemical potential is the sum of the chemical and electric potentials. Equation 1 can therefore be written as,

$$\mu'_{Na} + F\phi' = \mu''_{Na} + F\phi'' \tag{2}$$

where μ and ϕ denote chemical and electrical potential respectively and F is the Faraday constant. The open circuit e.m.f. E, is the difference of electrical potentials at the electrodes; hence

$$E = \phi'' - \phi' \tag{3}$$

Substituting equation 2 in 3 gives

$$E = \frac{\mu'_{Na} - \mu''_{Na}}{F} = \frac{RT}{F} \ln\left(\frac{a'_{Na}}{a''_{Na}}\right) \tag{4}$$

The chemical potential μ'_{Na}, and the corresponding sodium activity a'_{Na} at the anode is fixed by the dissociation reaction

$$Na_2SO_4 \longrightarrow 2\,Na + SO_3 + 1/2O_2 \tag{5}$$

as discussed by Jacob and Rao [2]. The equilibrium constant for reaction (5) is

$$K_5 = a^2_{Na'} p'_{SO_3} p'^{1/2}_{O_2} \tag{6}$$

Table 1. Measured cell potentials and response times

Temperature T, K	E.m.f E, mV(±1)	*Response time for 99% response* (min)	*Temperature* T, K	E.m.f. E, mV(±1)	*Response time for 99% response* (min)
Test gas 1			*Test gas 5*	773	202
29					
723	−240	39			
824	220	18	772	−220	26
871	238	15	901	−208	13
925	263	12	1010	−230	14
974	286	11	1077	−250	8
1026	309	10	967	−220	15
1072	312	10	821	−210	18
998	296	12			
913	258	13			
Test gas 2			*Test gas 10*		
772	168	30	772	−293	30
825	185	19	825	−308	20
873	200	16	924	−331	15
921	217	13	980	−343	12
1024	256	10	1025	−352	10
1076	275	9	1073	−364	8
984	242	11	843	−313	18
861	197	18			
794	176	24			
Test gas 3					
770	58	27			
828	65	18			
924	78	12			
1027	82	10			
1072	97	8			
873	70	15			
821	65	17			
772	58	29			

where p'_{SO_3} and p'_{O_2} are the partial pressures of SO_3 and O_2 respectively at the anode. The reverse reaction occurs at the cathode. The partial pressures p''_{SO_3} and p''_{O_2} fix the sodium activity a''_{Na} at the cathode. By substituting for the sodium activities the open circuit potential, E, in equation 4 becomes,

$$E = \frac{RT}{2F} \ln \left(\frac{p''_{SO_3} p''^{1/2}_{O_2}}{p'_{SO_3} p'^{1/2}_{O_2}} \right) \quad (7)$$

Since SO_3, SO_2 and O_2 are in equilibrium according to the reaction,

$$SO_3 \longrightarrow SO_2 + 1/2O_2 \quad (8)$$

the partial pressure p_{SO_3} can be written as

$$p_{SO_3} = \frac{p_{SO_2} p^{1/2}_{O_2}}{K_8} \quad (9)$$

where K_8 is the equilibrium constant for reaction (8). Combining equations 7 and 9,

$$E = \frac{RT}{2F} \ln \left(\frac{p''_{SO_2} p''_{O_2}}{p'_{SO_2} p'_{O_2}} \right) \quad (10)$$

when equilibrium exists in the gas phase. If the partial pressures of oxygen are equal at the two electrodes, the cell can be directly used to measure the concentrations of SO_3 (or SO_2 when equilibrium prevails in the gas) according to the relation:

$$E = \frac{RT}{2F} \ln \left(\frac{p''_{SO_3}}{p'_{SO_3}} \right) = \frac{RT}{2F} \ln \left(\frac{p''_{SO_2}}{p'_{SO_2}} \right) \quad (11)$$

For non-equilibrium gas mixtures the cell responds to the partial pressures of SO_3 and O_2 as discussed by Jacob and Rao [2].

4.2. *Calculation of the high temperature gas composition*

At the high temperatures of e.m.f. measurement, the gas composition will be altered due to the formation of SO_3 from SO_2 and O_2. The high temperature equilibrium gas composition was computed using values given in the literature [12] for the equilibrium constant (K_8) for reaction 8 and mass balance constraints [2]. Table 2 shows the inlet gas composition, the high temperature gas composition and the theoretical e.m.f. given by the Nernst equation. The calculations correspond to a total pressure of 1.01×10^5 Pa.

4.3. *E.m.f. studies*

The measured e.m.f.s were in good agreement with theoretically calculated values based on the Nernst equation, except for test gas 5, which showed systematic deviations of ~6 mV from the theoretical value. The consistent deviation of measured e.m.f.s at all

Table 2. Calculated high temperature equilibrium gas composition and the corresponding theoretical e.m.f. for the various test gas mixtures

Test gas No.	*Inlet composition*, vol %			*Temperature T*, K	*High temperature composition*, vol %				log ($p_{SO_3} p_{O_2}^{1/2}$)	Theoretical e.m.f. *E*, mV
	SO_2	O_2	Ar		SO_3	SO_2	O_2	Ar		
1	20.5	35.2	44.3	700	22.67	1.49×10^{-1}	27.85	49.33	−0.9221	183
				800	21.54	1.17	28.22	49.07	−0.9415	213
				900	17.50	4.79	29.53	48.18	−1.0218	252
				1000	10.94	10.68	31.66	46.72	−1.2107	297
				1100	5.60	15.47	33.38	45.55	−1.4901	339.5
2	11.2	18.1	70.7	700	11.75	1.12×10^{-1}	13.29	74.85	−1.3682	152
				800	10.96	8.56×10^{-1}	13.61	74.57	−1.3933	177
				900	8.41	3.27	14.66	73.67	−1.4921	210
				1000	4.84	6.63	16.12	72.41	−1.7115	247.5
				1100	2.34	8.995	17.14	71.53	−2.0138	282
3	0.79	4.91	94.3	700	7.86×10^{-1}	1.27×10^{-2}	4.54	94.67	−2.7760	54
				800	6.99×10^{-1}	9.41×10^{-2}	4.58	94.63	−2.8251	63
				900	4.69×10^{-1}	3.23×10^{-1}	4.68	94.54	−2.9937	76
				1000	2.25×10^{-1}	5.66×10^{-1}	4.80	94.41	−3.3072	89
				1100	9.60×10^{-2}	6.94×10^{-1}	4.684	94.35	−3.6742	101
4 *Ref. gas*	0.19	2.31	97.5	700	1.86×10^{-1}	4.33×10^{-3}	2.22	97.59	−3.5573	0
				800	1.59×10^{-1}	3.07×10^{-2}	2.23	97.58	−3.6245	0
				900	9.56×10^{-2}	9.45×10^{-2}	2.26	97.55	−3.8425	0
				1000	4.11×10^{-2}	1.49×10^{-1}	2.29	97.52	−4.2067	0
				1100	1.65×10^{-2}	1.735×10^{-1}	2.30	97.51	−4.6014	0
5	2.1×10^{-1}	9.2×10^{-3}	99.78	700	1.84×10^{-2}	1.92×10^{-1}	1.11×10^{-5}	99.79	−7.2125	−254
				800	1.71×10^{-2}	1.93×10^{-1}	6.52×10^{-4}	99.79	−6.3599	−217
				900	9.17×10^{-3}	2.01×10^{-1}	4.61×10^{-3}	99.79	−6.2057	−211
				1000	3.27×10^{-3}	2.07×10^{-1}	7.56×10^{-3}	99.78	−6.5462	−232
				1100	1.21×10^{-3}	2.09×10^{-1}	8.59×10^{-3}	99.78	−6.9502	−256
10	8.2×10^{-6}	24.4	75.599	700	8.143×10^{-6}	5.714×10^{-8}	24.40	75.60	−7.3955	−266.5
				800	7.75×10^{-6}	4.52×10^{-7}	24.40	75.60	−7.4170	−301
				900	6.30×10^{-6}	1.898×10^{-6}	24.40	75.60	−7.5070	−327
				1000	3.88×10^{-6}	4.32×10^{-6}	24.40	75.60	−7.7175	−348
				1100	1.94×10^{-6}	6.26×10^{-6}	24.40	75.60	−8.0185	−373

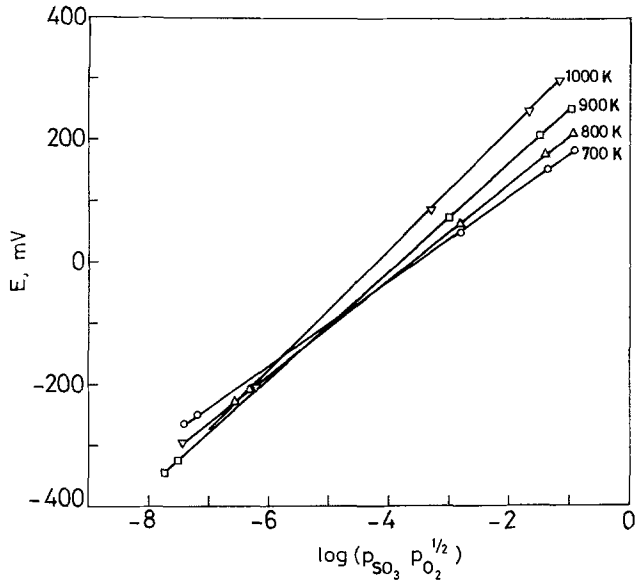

Fig. 4. Variation of the theoretical e.m.f. with log ($p_{SO_3}p_{O_2}^{1/2}$) at different temperatures.

temperatures suggests the possibility of a small error in the determination of the composition of test gas No. 5. Only two experimental points, one at 1027 K corresponding to test gas No. 3 and another at 1072 K corresponding to test gas No. 1 gave e.m.f.s lower by more than 10 mV than that calculated from equation 7. The good agreement of the experimental results with the Nernstian values confirmed that equilibrium between SO_3, SO_2 and O_2 was attained in the gas phase and the sensor functions satisfactorily for SO_x.

The e.m.f. is plotted as a function of log (p_{SO_3} $p_{O_2}^{1/2}$) in Fig. 4 at regular intervals of temperature. The points are obtained by interpolation from experimental data shown in Figs. 1 and 2. The plots are linear. The slope for each temperature corresponds to the theoretical value of 2.303 RT/2F. The variation of log ($p_{SO_3}p_{O_2}^{1/2}$) with temperature is shown in Fig. 5. The non-linearity of plots in Figs 1 and 2 is therefore due to a non-linear variation with temperature of the function log (p_{SO_3} $p_{O_2}^{1/2}$) for a fixed inlet gas composition, especially at low and unequal concentrations of SO_2 and O_2.

The e.m.f. of the cell depends on the product of the partial pressures of SO_3 and O_2 raised to the power one half, or SO_2 and O_2, as given by equations 7 and 10, respectively. To obtain the absolute value of p_{SO_3} or p_{SO_2}, the partial pressure of oxygen should be independently measured. Thus, if the sensor is to be used to monitor SO_2 or SO_3 species, it should be coupled with an oxygen sensor, or the chemical potential of oxygen should be the same at both electrodes.

The lowest partial pressure of SO_3 that can be measured by a sensor based on Nasicon is determined by the decomposition of Na_2SO_4 according to the reaction:

$$Na_2SO_4(s) \longrightarrow SO_3(g) + Na_2O(\text{Nasicon}) \quad (12)$$

Using standard thermodynamic data for Na_2SO_4, $SO_3(g)$ and Na_2O [13] and activity of Na_2O in $Na_3Zr_2Si_2PO_{12}$ [14],

$$\log a_{Na_2O} = -\frac{12050}{T} - 2.15 \quad (13)$$

the lowest partial pressure limit can be evaluated as $p_{SO_3} \approx 4.53 \times 10^{-8}$ atm. at 1000 K.

4.4. *Advantages of Nasicon electrolyte*

The Nasicon materials belong to a solid solution series originally represented as $Na_{1+x}Zr_2P_{2-x}Si_xO_{12}$ [15]. More recently, single crystal X-ray diffraction studies [16] have shown that Nasicon belongs to a solid solution series more correctly represented by

$$Na_{1+z}Zr_{2-y}Si_xP_{3-x}O_{12};\ z - x - 4y = 0$$

The parameters x, y and z are limited by valence compensation and structural features to

$$0 \leqslant x \leqslant 3,\quad 0 \leqslant y \leqslant 3/4,\quad 0 \leqslant z \leqslant 3$$

The value of the ionic conductivity for $Na_3Zr_2Si_2PO_{12}$ at 720 K is $\sim 37.5\ (\Omega\text{cm})^{-1}$ [11]. This is to be compared with ionic conductivities of $\sim 7.8 \times 10^{-5}$

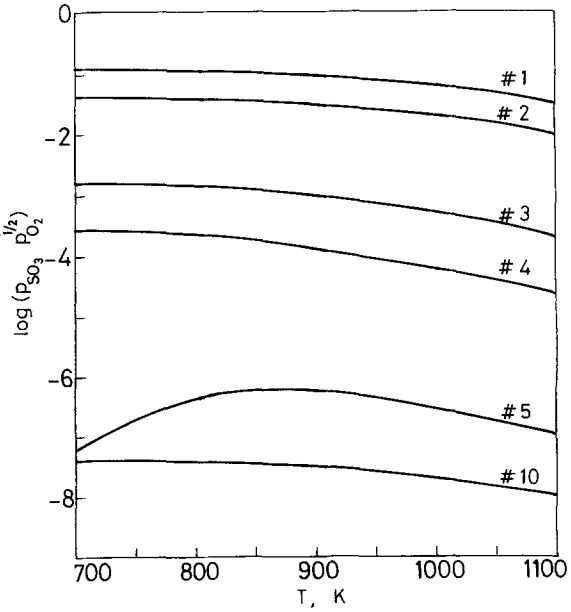

Fig. 5. Temperature dependence of log ($p_{SO_3}p_{O_2}^{1/2}$) for different inlet gas compositions.

$(\Omega\,cm)^{-1}$ for Na_2SO_4 – I [2] and $\sim 10^{-6}\,(\Omega\,cm)^{-1}$ for orthorhombic K_2SO_4 [17] at 720 K. The higher conductivity of Nasicon at lower temperatures is an important factor favouring its use in sensors designed for operation at lower temperatures. The response times with pure Nasicon [6] are of the same order of magnitude as for Na_2SO_4 – I at high temperatures [2]. This suggests that response time is not controlled by the bulk properties of the solid electrolyte. The electrode reactions are probably rate controlling. These reactions are the same in cells using Nasicon and Na_2SO_4 as electrolytes, since the latter is always formed at the Nasicon/gas interface. When Nasicon is used in conjunction with Na_2SO_4 – I, the intrinsic response time at 723 K is ~ 2.0 ksec, too large for most applications. The lower temperature limit for commercial operation of a sensor based on the response time is ~ 950 K. Although a phase transformation from monoclinic to rhombohedral symmetry occurs in Nasicon at ~ 423 K, it is not accompanied by a large volume change that causes structural deterioration as in the case of alkali sulphates. If a cell containing only the Nasicon solid electrolyte is thermally cycled through the phase transformation temperature for Na_2SO_4, the protective layer of Na_2SO_4 will develop cracks allowing access of the gas to the electrolyte. Since Nasicon is not chemically stable against SO_x gas species, there will be chemical deterioriation of the solid electrolyte over long exposures. The Nasicon/Na_2SO_4 couple used in this study combines the mechanical stability of Nasicon with the chemical stability of Na_2SO_4 against SO_x gas species.

Acknowledgements

The authors acknowledge the assistance of Mrs R. Sarojini and Mr A. V. Narayan in the preparation of the manuscript.

References

[1] M. Gauthier and A. Chamberland, *J. Electrochem. Soc.* **124** (1977) 1579.
[2] K. T. Jacob and D. B. Rao, *ibid.* **126** (1979) 1842.
[3] Q. G. Liu and W. L. Worrell in 'Chemical Metallurgy – A tribute to Carl Wagner', edited by N. A. Gokcen. The Metallurgical Soc., AIME, Warrendale (1981) p. 43.
[4] W. L. Worrell and Q. G. Liu, *Sensors and Actuators*, **2** (1982) 385.
[5] *Idem, J. Electroanal. Chem.* **168** (1984) 355.
[6] Y. Saito, T. Maruyama, Y. Matsumoto, K. Kobayashi and Y. Yano, *Solid State Ionics* **14** (1984) 273.
[7] M. Gauthier, R. Bellemare and A. Belanger, *J. Electrochem. Soc.* **128** (1981) 371.
[8] K. T. Jacob and G. N. K. Iyengar, *Metall. Trans. B.* **17B** (1986) 323.
[9] N. Imanaka, Y. Yamaguchi, G. Adachi and J. Shioka, *J. Electrochem. Soc.* **133** (1986) 1026.
[10] K. T. Jacob, M. Iwase and Y. Waseda, *Solid State Ionics* **23** (1987) 245.
[11] T. Maruyama, Y. Saito, Y. Matsumoto and Y. Yano, *ibid.* **17** (1985) 281.
[12] D. R. Stull and H. Prophet in 'JANAF Thermochemical Tables' 2nd edn. NSRDS-NBS 37, US Dept. of Commerce, Washington D.C. (1971).
[13] L. B. Pankratz, J. M. Stuve and N. A. Gokcen, in 'Thermodynamic Data for Mineral Technology', US Bur. Mines, Bulletin 677, US Dept. of the Interior, Washington, DC (1984).
[14] G. M. Kale and K. J. Jacob, *J. Mater. Res.*, submitted for publication.
[15] J. B. Goodenough, H. Y. P. Hong and J. A. Kafalas, *Mat. Res. Bull.* **11** (1976) 203.
[16] H. Kohler, H. Schulz and O. Melnikov, *ibid.* **18** (1983) 1143.
[17] M. Natarajan and E. A. Secco, *Can. J. Chem.* **53** (1975) 1542.